Effects of Covalent Modifications on the Solid-State Folding and Packing of *N*-Malonylglycine Derivatives

Gregory P. Dado, John M. Desper, Steven K. Holmgren, Christopher J. Rito, and Samuel H. Gellman*

Contribution from the S. M. McElvain Laboratory of Organic Chemistry, Department of Chemistry, University of Wisconsin, 1101 University Avenue, Madison, Wisconsin 53706.
Received September 27, 1991

Abstract: The syntheses and crystal structures of triamides **1**–**4** and diamide esters **5** and **6** are described. In crystalline form, **1**, **2**, and **4** adopt conformations containing an intramolecular N—H···O=C hydrogen bond in a nine-membered ring. Triamide **3** and ester diamides **5** and **6** experience only intermolecular hydrogen bonding in the solid state. We have previously concluded, on the basis of IR and ^{1}H NMR measurements, that triamide **1** manifests several different internal hydrogen-bonding patterns in methylene chloride solution. The conformation adopted by **1** in the solid state is similar to the folding pattern that we earlier deduced to be most enthalpically favorable in nonpolar solution, although an intermolecular hydrogen bond detected in the crystalline **1** does not occur at the dilutions used for the solution experiments. The intramolecularly hydrogen-bonded solid-state conformations of **2** and **4** are similar to those that predominate in methylene chloride solution. In contrast, the extended, intermolecularly hydrogen-bonded conformation of **3** in the solid state differs from the intramolecularly hydrogen-bonded form that is favored in dilute methylene chloride. The solid-state conformations of diamide esters **5** and **6** also differ from the forms that appear to be most highly populated in nonpolar solution. The crystal packing of **2**–**4** is discussed in detail. Although the juxtapositions of neighbors vary among these triamides, in all three cases a pattern of alternating sheets of polar and nonpolar fragments is observed.

Introduction

The structural roles played by noncovalent interactions continue to be a source of interest to researchers examining the folding of biopolymers,[1] the recognition of one molecule by another in solution,[2] and the control of long-range order in the solid state.[3] We have been exploring the interplay of noncovalent forces that influences the adoption of folded conformations by small synthetic oligoamides.[4,5] These experiments are of intrinsic interest in the realm of physical organic chemistry, and they constitute model studies that provide insight on the networks of interlocking nonbonded interactions that determine the secondary structural preferences of proteins. In preliminary communications, we have reported that dipeptide analogues derived from *N*-malonylglycine display a marked tendency to fold back upon themselves, with concomitant formation of an intramolecular N—H···O=C hydrogen bond in a nine-membered ring.[5] We now describe in full the synthesis and crystallography of triamides **1**–**4** and diamide esters **5** and **6**.

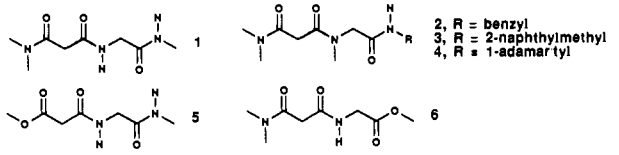

Results and Discussion

Triamides **1**–**4** were prepared using standard peptide-coupling methodology,[6] as outlined in Scheme I. Diamide esters **5** and **6** were synthesized by similar procedures; details may be found in the Experimental Section. The crystalline conformations of **1**–**6** are shown in Figures 1–6; the numbering scheme employed for these molecules is indicated in Figure 7. There are two independent molecules in crystallline **4** and **5**. The two conformations of **4** are almost indistinguishable, and only one form is shown in Figure 4. The two conformations of **5** have significant variations in several backbone torsion angles; both forms are shown in Figure 5.

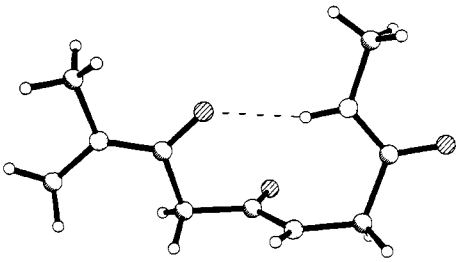

Figure 1. Ball-and-stick representation of triamide **1** in the crystalline state. The intramolecular N—H···O=C hydrogen bond is indicated by a dotted line. An intermolecular hydrogen bond involving H_9 and O_{12} is not shown. The atomic numbering system is given in Figure 7.

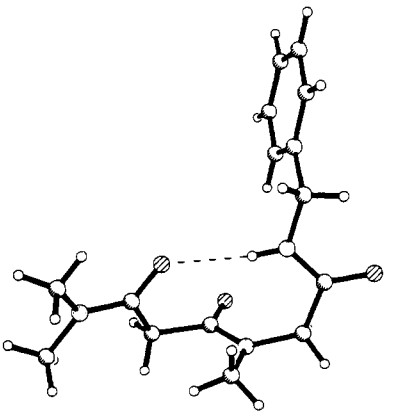

Figure 2. Ball-and-stick representation of triamide **2** in the crystalline state. The intramolecular N—H···O=C hydrogen bond is indicated by a dotted line. The atomic numbering system is given in Figure 7.

Intramolecular N—H···O=C hydrogen bonds occurring in crystalline **1**, **2**, and **4** and intermolecular N—H···O=C hydrogen

(1) Dill, K. A. *Biochemistry* **1990**, *29*, 7133 and references therein.
(2) Rebek, J. *Angew. Chem., Int. Ed. Engl.* **1990**, *29*, 245 and references therein.
(3) (a) Etter, M. C. *Acc. Chem. Res.* **1990**, *23*, 120. (b) Etter, M. C. *J. Phys. Chem.* **1991**, *95*, 4601 and references therein.
(4) Gellman, S. H.; Dado, G. P.; Liang, G.-B.; Adams, B. R. *J. Am. Chem. Soc.* **1991**, *113*, 1164.
(5) Gellman, S. H.; Adams, B. R.; Dado, G. P. *J. Am. Chem. Soc.* **1990**, *112*, 460. (b) Dado, G. P.; Desper, J. M.; Gellman, S. H. *J. Am. Chem. Soc.* **1990**, *112*, 8630. (c) Liang, G.-B.; Dado, G. P.; Gellman, S. H. *J. Am. Chem. Soc.* **1991**, *113*, 3994.
(6) Bodanszky, M.; Bodanszky, A. *The Practice of Peptide Synthesis*; Springer-Verlag: Berlin, 1984.

0002-7863/92/1514-4834$03.00/0

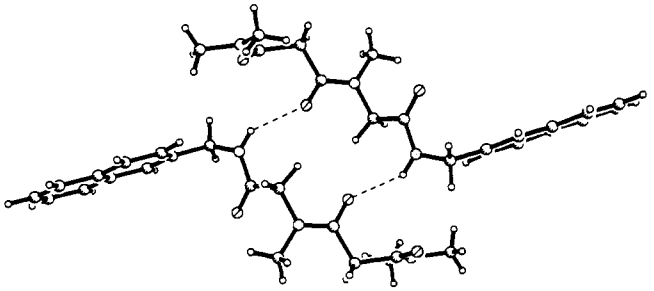

Figure 3. Ball-and-stick representation of triamide **3** in the crystalline state. The intermolecularly N—H···O═C hydrogen-bonded dimer is shown; the N—H···O═C interactions are indicated by dotted lines. The atomic numbering system is given in Figure 7.

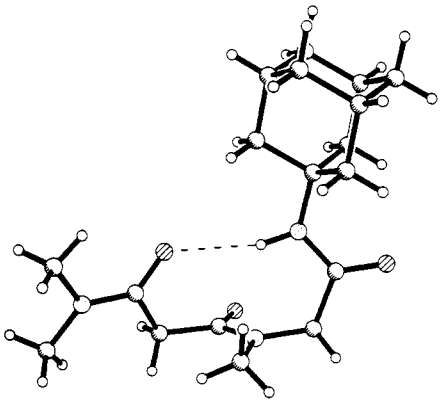

Figure 4. Ball-and-stick representation of triamide **4** in the crystalline state. The intramolecular N—H···O═C hydrogen bond is indicated by a dotted line. The two independent molecules in the lattice have nearly identical conformations, and only one is shown. The atomic numbering system is given in Figure 7.

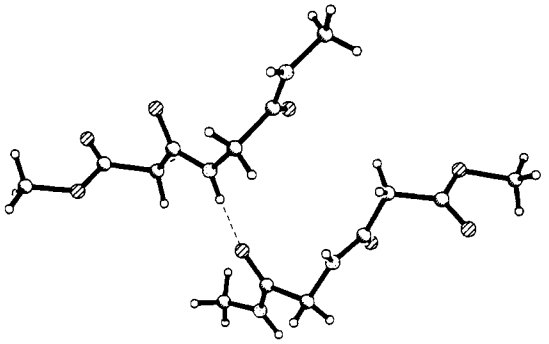

Figure 5. Ball-and-stick representation of diamide ester **5** in the crystalline state. Both of the independent molecules found in lattice are shown. As indicated in Table III, there are four distinct intermolecular N—H···O═C hydrogen bonds in the crystal lattice of **5**; only one of these interactions is shown here, indicated by a dotted line. The atomic numbering system is given in Figure 7.

bonds occurring in crystalline **3**, **5**, and **6** are indicated in Figures 1–6. Although not shown in Figure 1, an intermolecular N—H···O═C interaction occurs in crystalline **1** involving O_{12} and H_9. Only a single type of intermolecular N—H···O═C pairing is observed for **3** and **6**, but there are four distinct intermolecular N—H···O═C pairings in crystalline **5**, only one of which is shown.

Table III summarizes the N—H···O═C geometries observed in these crystal structures. The amide protons of **1**–**4** and **6** were

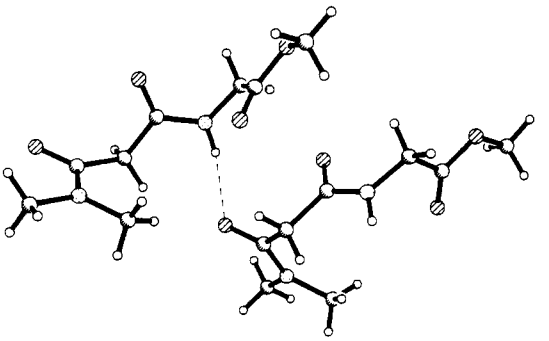

Figure 6. Ball-and-stick representation of diamide ester **6** in the crystalline state. Two molecules are shown to illustrate the intermolecular N—H···O═C hydrogen bond, which is indicated by a dotted line. The atomic numbering system is given in Figure 7.

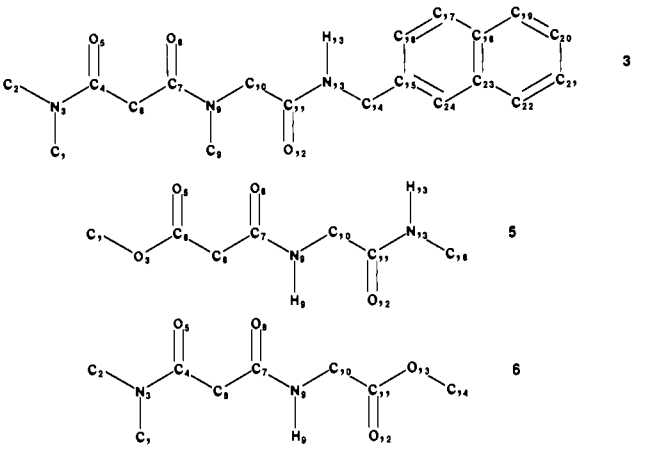

Figure 7. Atomic numbering scheme used for **1**–**6**. The triamide fragment common to **1**–**4** is numbered as shown for **3**; for **1**, the hydrogen on N_9 is H_9.

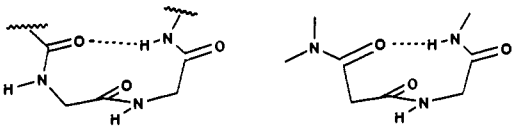

Figure 8. A schematic comparison of the β-turn folding pattern of a Gly-Gly segment with the nine-membered-ring hydrogen-bonded folding pattern of triamide **1**.

refined independently during the structure determination. The crystallographic data set for **5** is not large enough for independent refinement of the amide proton positions, and the values given for **5** in Table III are based on assumed positions of the hydrogen atoms. Selected torsion angles for **1**–**6** are provided in Tables IV and V. The C_7N_9—$C_{10}C_{11}$ torsion angles reported in Tables IV and V correspond to the ϕ torsion angle conventionally reported for glycine residues, and the N_9C_{10}—$C_{11}N_{13}$ torsion angles (N_9C_{10}—$C_{11}O_{13}$ for **6**) in the tables correspond to the glycine ψ torsion angles.

Molecular Folding Patterns. The intramolecularly hydrogen-bonded conformation observed for **1** is related to a β-turn formed across a Gly-Gly sequence (Figure 8). The hydrogen-bonded ring of **1** is smaller than that observed in β-turns (nine- vs ten-membered) because, in effect, the first glycine residue's nitrogen atom is removed from the hydrogen-bonded ring of **1**. Viewed in this light, the ϕ and ψ angles of the Gly residue in the nine-membered ring of **1** should be compared with the corresponding

Scheme I

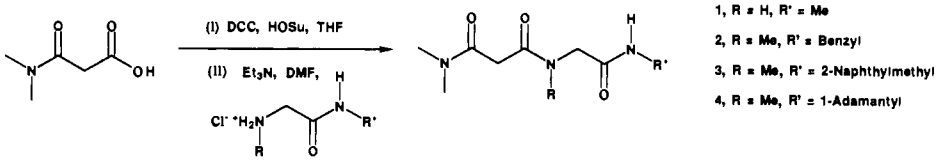

Table I. Data Collection and Refinement for Triamides **1–4**

	1	2	3	4
formula	$C_8H_{15}N_3O_3$	$C_{15}H_{21}N_3O_3$	$C_{19}H_{23}N_3O_3$	$C_{18}H_{29}N_3O_3$
MW	201.2	291.3	341.4	335.4
cryst size, mm	0.4 × 0.3 × 0.2	0.3 × 0.2 × 0.2	0.4 × 0.3 × 0.3	0.5 × 0.2 × 0.05
cryst syst	orthorhombic	orthorhombic	monoclinic	triclinic
space group	$P2_12_12_1$	$P2_12_12_1$	$P2_1/a$	$P\bar{1}$
a, Å	8.207 (3)	6.173 (3)	16.951 (6)	11.145 (2)
b, Å	8.617 (3)	8.676 (5)	5.682 (2)	12.372 (3)
c, Å	14.590 (5)	28.581 (13)	18.015 (7)	13.807 (3)
α, deg				75.20 (2)
β, deg			99.36 (3)	88.283 (15)
γ, deg				83.07 (2)
vol, Å^3	1031.8 (6)	1530.6 (13)	1712.1 (11)	1827.2 (7)
Z	4	4	4	4
D_{calcd}, g/cm^3	1.295	1.264	1.324	1.219
$F(000)$	432	624	728	728
λ	Cu Kα	Cu Kα	Mo Kα	Cu Kα
μ, cm^{-1}	8.04	6.94	0.85	6.37
temp, K	95	93	95	93
2θ range, deg	3.5–110	3.5–110	3.5–50	3.0–110
scan technique	ω	ω	2θ–θ	Wyckoff
scan range, deg	1.4	1.4	1.8 + Kα sepn	0.7
scan speed, deg/min	3–30	2–30	2–20	3–30
reflns collected	756	1082	3488	4580
unique reflns	719	1057	2876	4578
R_{merg}			8.62	
reflns obsd	697	1018	1947	3656
R/R_w (obsd data)	3.25/4.30	3.63/4.60	6.64/8.46	6.70/8.35
R/R_w (all data)	3.56/4.76	3.82/4.69	9.95/10.01	8.46/8.90
S	1.77	1.94	1.88	2.62
$\Delta\rho_{max/min}$, e/Å^3	0.11/–0.17	0.12/–0.22	0.27/–0.28	0.25/–0.28
data:param ratio	4.8:1	5.0:1	7.7:1	7.9:1

Table II. Data Collection and Refinement for Diamide Esters **5** and **6**

	5	6
formula	$C_7H_{12}N_2O_4$	$C_8H_{14}N_2O_4$
MW	188.2	202.2
cryst size, mm	0.4 × 0.2 × 0.05	0.4 × 0.2 × 0.1
cryst syst	monoclinic	monoclinic
space group	$P2_1$	$P2_1/c$
a, Å	8.345 (2)	7.183 (3)
b, Å	9.400 (2)	14.042 (5)
c, Å	12.433 (2)	9.924 (3)
β, deg	100.096 (2)	100.10 (3)
vol, Å^3	959.5 (3)	985.5 (6)
Z	4	4
D_{calcd}, g/cm^3	1.303	1.363
$F(000)$	400	432
λ	Cu Kα	Cu Kα
μ, cm^{-1}	8.76	8.88
temp, K	298	113
2θ range, deg	3.5–110	3.5–114
scan technique	ω	Wyckoff
scan range, deg	2.2	1.0
scan speed, deg/min	2–20	2–20
reflns collected	1748	1400
unique reflns	1270	1328
R_{merg}	5.20	
reflns obsd	945	1167
R/R_w (obsd data)	6.04/6.41	4.15/5.82
R/R_w (all data)	8.49/7.02	4.70/5.91
S	1.77	2.02
$\Delta\rho_{max/min}$, e/Å^3	0.20/–0.21	0.23/–0.19
data:param ratio	4.0:1	8.3:1

torsion angles of Gly residues observed in the third position ("i + 2") of β-turns. Statistical analysis of the protein crystal structure database shows that Gly is particularly prevalent at the third position of type II β-turns,[7] and the ideal Gly torsion angles in this position are commonly assumed to be $\phi = 80°$ and $\psi = 0°$.[8] The corresponding values for **1** are quite similar (74.0 (3)° and 4.3 (3)°), as are the analogous torsion angles observed for the *N*-methylglycine (sarcosine) residues contained in the folded conformations of **2** and **4**. The ϕ,ψ angles for the extended conformations of **3**, **5**, and **6** correspond reasonably well to the ideal polyglycine II values (–80°,150°)[9] and to the ϕ,ψ angles reported for crystalline acetylglycine *N*-methylamide.[10]

Considerably fewer data are available on the conformational preferences of malonic acid-derived diamides than for α-amino acid residues.[11] In most known structures of malonamide derivatives, the planes of the two amide groups are approximately perpendicular to one another, unless a six-membered-ring hydrogen bond occurs. (Of eleven conformationally mobile malonamide derivatives bearing at least one amide proton located in the Cambridge Structural Database, five display a six-membered-ring hydrogen bond and six experience only intermolecular hydrogen bonding.[12]) If we consider triamides **1–4** in terms of the Gly-Gly analogy mentioned above, then we can define ϕ' and ψ' torsion angles for the malonamide fragments as N_3C_4–C_6C_7 and C_4–C_6–C_7N_9, respectively. The ϕ',ψ' patterns for **1**, **2**, and **4** are similar and lead to approximate orthogonality between the amide planes. Although the ϕ',ψ' values are more varied among the extended conformations adopted by **3**, **5**, and **6**, the tendency toward orthogonal amide planes is maintained in all cases.

El Masourdi et al. have reported crystal structures for two triamides related to **1–6**.[13] Both **7** and **8** adopt extended con-

(7) (a) Chou, P. Y.; Fasman, G. D. *J. Mol. Biol.* **1977**, *115*, 135. (b) Chou, P. Y.; Fasman, G. D. *Biophys. J.* **1979**, *26*, 367.

(8) Rose, G. D.; Gierasch, L. M.; Smith, J. A. *Adv. Protein Chem.* **1985**, *37*, 1.

(9) IUPAC-IUB Comm. Report on Biochemical Nomenclature. *J. Mol. Biol.* **1970**, *52*, 1.

(10) Iwasaki, F. *Acta Crystallogr.* **1974**, *B30*, 2503.

(11) Malonic acid residues have been incorporated into peptide analogues that are referred to as "retro-inverso peptides", see: Goodman, M.; Chorev, M. *Acc. Chem. Res.* **1979**, *12*, 1 and references therein.

(12) Cambridge Structural Database version 4.4 (January 1991); Allen, F. H.; Kennard, O.; Taylor, R. *Acc. Chem. Res.* **1983**, *16*, 46. Literature citations for the 11 structures located are provided in the supplementary material. If we include compounds **7** and **8** of Masourdi et al. (ref 13) and our compounds **1** and **6** in our reckoning, there are crystal structures available for 15 malonamide derivatives, only five of which show a six-membered-ring hydrogen bond in the solid state.

(13) El Masourdi, L.; Aubry, A.; Gomez, E. J.; Vitoux, B.; Marraud, M. *J. Chim. Phys.* **1988**, *85*, 583.

Table III. Geometrical Parameters for N—H···O=C Hydrogen Bonds Observed in the Crystal Lattices of **1–6**

molecule	H-bond	O···H,[a] Å	N···O,[b] Å	angle at H,[c] deg	angle at O,[d] deg	out-of-plane,[e] deg
1	O_5–H_{13}	2.08 (4)	2.956 (4)	165 (3)	129 (1)	1
	O_{12}–H_9[f]	1.87 (4)	2.811 (4)	178 (3)	131 (1)	27
2	O_5–H_{13}	2.20 (4)	3.016 (4)	167 (2)	130 (1)	28
3	O_8–H_{13}[f]	2.19 (4)	2.970 (6)	142 (4)	131 (1)	48
4	O_5–H_{13}	2.28 (4)	3.210 (6)	165 (4)	127 (1)	25
	O_5–H_{13}	2.27 (4)	3.110 (6)	164 (4)	128 (1)	32
5	O_8–H_9[f]	1.94 (1)	2.835 (11)	174 (1)	166 (1)	10
	O_8–H_{13}[f]	1.94 (2)	2.839 (16)	175 (1)	155 (1)	2
	O_{12}–H_9[f]	1.91 (1)	2.790 (13)	166 (1)	152 (1)	12
	O_{12}–H_{13}[f]	1.90 (2)	2.793 (17)	175 (1)	167 (1)	31
6	O_5–H_9[f]	2.08 (3)	2.950 (3)	166 (3)	116 (1)	38

[a] O···H distance; the relevant H atoms were independently refined for **1–4** and **6**. The hydrogen atom positions are assumed for **5**. [b] Distance between N of the hydrogen bond donor and O of the acceptor. [c] Angle formed by N—H···O. [d] Angle formed by C=O···H. [e] Angle between the planes defined by C=O···H and N—C=O of the hydrogen-bond-acceptor amide. [f] Intermolecular hydrogen bond (all others are intramolecular hydrogen bonds).

Table IV. Selected Torsion Angles for Triamides **1–4**

angle	**1**, deg	**2**, deg	**3**, deg	**4**, deg	
C1–N3–C4–O5	174.0 (3)	−178.1 (3)	175.1 (4)	1.9 (7)	−176.4 (4)
C1–N3–C4–C6	−6.8 (4)	2.1 (4)	−5.5 (6)	−177.4 (4)	3.0 (6)
C2–N3–C4–O5	2.7 (4)	−11.2 (5)	−0.2 (6)	−177.3 (4)	−1.4 (6)
C2–N3–C4–C6	−178.1 (3)	169.0 (3)	179.2 (4)	3.5 (6)	178.0 (4)
N3–C4–C6–C7	170.4 (3)	−166.9 (3)	89.4 (5)	165.0 (4)	160.5 (4)
O5–C4–C6–C7	−10.4 (4)	13.4 (4)	−91.1 (5)	−14.3 (6)	−20.1 (5)
C4–C6–C7–O8	−94.4 (3)	−110.9 (3)	−22.2 (5)	116.4 (5)	115.2 (4)
C4–C6–C7–N9	84.3 (3)	69.2 (3)	157.2 (3)	−63.4 (5)	−65.2 (4)
C6–C7–N9–C10	−173.4 (3)	−172.9 (3)	−172.8 (3)	−176.6 (4)	172.5 (3)
O8–C7–N9–C10	5.3 (4)	7.1 (4)	6.6 (5)	−3.2 (7)	−7.9 (5)
C7–N9–C10–C11	74.0 (3)	89.4 (3)	−102.6 (4)	−93.5 (5)	−91.2 (4)
N9–C10–C11–O12	−177.1 (3)	169.9 (3)	−20.6 (6)	−169.3 (3)	−167.1 (3)
N9–C10–C11–N13	4.3 (4)	−10.2 (4)	163.6 (3)	11.4 (5)	14.2 (5)
C10–C11–N13–C14	178.5 (2)	−178.3 (3)	171.0 (4)	−176.0 (3)	175.3 (3)
O12–C11–N13–C14	0.1 (4)	1.6 (5)	−4.8 (6)	4.8 (6)	−3.2 (6)

Table V. Selected Torsion Angles for Diamide Esters **5** and **6**

angle	**5**, deg		**6**, deg
C1–O3–C4–O5	−3.8 (13)	1.6 (14)	
C1–N3–C4–O5			178.6 (2)
C1–O3–C4–C6	177.4 (7)	−179.6 (8)	−1.3 (3)
C2–O3–C4–O5			0.7 (3)
C2–O3–C4–C6			−179.2 (2)
O3–C4–C6–C7	−72.3 (15)	106.6 (14)	81.9 (3)
O5–C4–C6–C7	108.9 (15)	−74.6 (16)	−98.0 (2)
C4–C6–C7–O8	−39.0 (22)	−57.4 (21)	35.9 (3)
C4–C6–C7–N9	145.5 (16)	124.4 (15)	−148.0 (2)
C6–C7–N9–C10	174.1 (14)	178.9 (14)	−179.8 (2)
O8–C7–N9–C10	−1.3 (25)	0.8 (25)	−3.8 (4)
C7–N9–C10–C11	−80.8 (16)	−78.1 (15)	−77.5 (3)
N9–C10–C11–O12	−20.4 (21)	−34.3 (19)	−4.8 (3)
N9–C10–C11–N13	156.4 (14)	147.7 (12)	
N9–C10–C11–O13			175.6 (2)
C10–C11–N13–C14	176.7 (15)	176.1 (14)	
C10–C11–O13–C14			−179.4 (2)
O12–C11–N13–C14	−6.7 (27)	−1.9 (25)	
O12–C11–O13–C14			1.0 (3)

formations in the solid state; only intermolecular hydrogen bonding occurs. On the basis of their crystallographic observations, these authors concluded that "the β-turn structure, characterized by a ten-membered chelation ring in peptides, is not compatible with the decrease to nine atoms in the chelation ring." The solid-state conformations of **1**, **2**, and **4**, as well as the behavior of **1–4** in solution, demonstrate this conclusion to be incorrect.

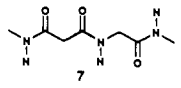

7

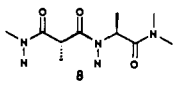

8

Hydrogen-Bonding Patterns and Geometry. In accord with the general rules proposed by Etter for hydrogen bonding among organic molecules in the solid state,[3] the maximum number of N—H···O=C interactions occurs for each of the molecules discussed here. Diamide esters **5** and **6** show further agreement with Etter's rules in that the amide protons hydrogen bond exclusively to the strongest acceptors, i.e., amide rather than ester carbonyls. A tendency for six-membered-ring intramolecular hydrogen bonds to form in preference to intermolecular hydrogen bonds has been noted in the solid state for a variety of types of compounds.[3] In this regard, it is interesting that neither **1**, **5**, nor **6** experiences a six-membered-ring hydrogen bond in its crystalline form. As mentioned above, other examples in the limited pool of relevant structures indicate that six-membered-ring hydrogen bonds are observed in the solid state for only a minority of malonamide derivatives.[12]

Table III reveals that most of the N—H···O=C interactions observed in crystalline **1–6** are significantly longer than the typical value of 1.95 Å.[14,15] Exceptions are the intermolecular hydrogen bond in **1**, 1.87 (4) Å, and the four intermolecular hydrogen bonds in **5**, 1.90–1.94 Å. Statistical analysis of all types of N—H···O=C interactions in small molecules indicates that intramolecular hydrogen bonds tend to be longer than analogous intermolecular hydrogen bonds,[14] and triamides **1**, **2**, and **4** fit this pattern. The H_{13}···O_5 lengths in adamantyl derivative **4** are particularly long (2.27 (4) and 2.28 (4) Å in the independent molecules), approaching the commonly used cutoff value for defining O···H hydrogen bonds from X-ray diffraction data (2.4 Å).[14] One possible rationale for the extreme length of these hydrogen bonds would be an unfavorably close intramolecular approach of O_5 to the nearest adamantyl hydrogens in the folded conformation; however, unfavorable steric interactions of this type are not detected crystallographically. The shortest adamantyl H···O_5 distances fall in the range 2.8–3.2 Å (the adamantyl hydrogen

(14) (a) Taylor, R.; Kennard, O. *Acta Crystallogr.* **1983**, *B39*, 133. (b) Taylor, R.; Kennard, O.; Versichel, W. *J. Am. Chem. Soc.* **1983**, *105*, 5761. (c) Taylor, R.; Kennard, O.; Versichel, W. *Acta Crystallogr.* **1984**, *B40*, 280.

(15) (a) Baker, E. N.; Hubbard, R. E. *Prog. Mol. Biol. Biophys.* **1984**, *44*, 97. (b) Ippolito, J. A.; Alexander, R. S.; Christianson, D. W. *J. Mol. Biol.* **1990**, *215*, 457.

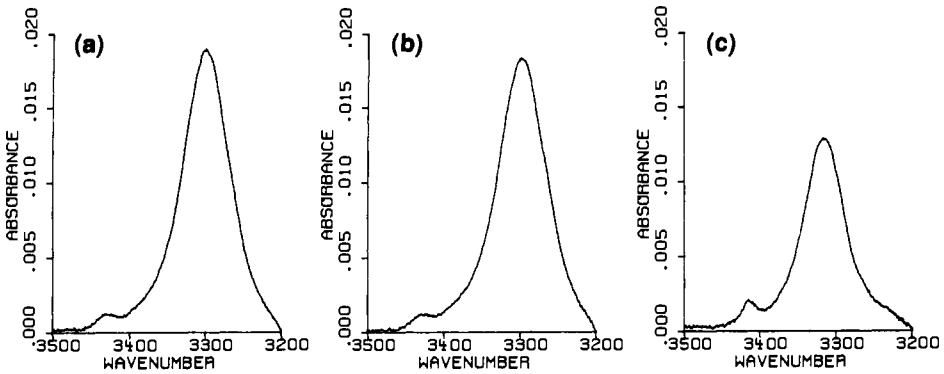

Figure 9. N–H stretch region of the FT-IR spectra for 1 mM triamide solutions in CH_2Cl_2 (room temperature), after subtraction of the spectrum of pure CH_2Cl_2. Data were obtained on a Nicolet 740 spectrometer: (a) triamide **2** (maxima at 3430 and 3299 cm^{-1}); (b) triamide **3** (maxima at 3430 and 3298 cm^{-1}); (c) triamide **4** (maxima at 3413 and 3316 cm^{-1}).

positions were not independently refined), which is larger than the sum of the oxygen and hydrogen van der Waals radii.

The intramolecular N—H···O=C interactions in **1**, **2**, and **4** all have angular features in the expected ranges,[14-16] with N—H···O angles 164–167°, C=O···H angles 127–131°, and out-of-plane distortions 1–32° (Table III). The intermolecular hydrogen bonds in crystalline **1**, **5**, and **6** also show typical angles. The intermolecular O_8···H_{13} hydrogen bond in **3**, however, has a suboptimal geometry in all important respects, with the N—H···O angle deviating significantly from linearity and the proton showing the largest out-of-plane distortion among the interactions reported here. This intermolecular hydrogen bond is also quite long. The unusual geometric features of the intermolecular N_{13}—H_{13}··· O_8=C_7 interaction observed in crystalline **3** may result in part from the involvement of O_8 in a weak attractive interaction with one of the hydrogen atoms on C_{10} of the same neighbor. The O···H distance of 2.34 (4) Å is within the range that has been proposed for the identification of C—H···O hydrogen bonds in crystal structures.[17]

Hydrogen-bond geometry provides at least a partial rationale for the apparent superiority of the nine-membered-ring interaction over alternative six- and/or seven-membered-ring hydrogen bonds. Crystallographically observed six-membered hydrogen-bonded rings analogous to those available to **1**, **5**, and **6** are characterized by decidedly nonlinear N–H···O arrangements (≤140°).[12] The seven-membered-ring hydrogen bond available to **1–5** corresponds to the γ-turn, a rare feature of protein secondary structure;[18] γ-turn hydrogen bonds observed in crystalline proteins deviate substantially from linearity (Baker and Hubbard[15a] reported a mean γ-turn N–H···O angle of 137°). Seven-membered-ring hydrogen bonds have apparently never been observed crystallographically in small acyclic peptides, although they have been detected in a number of small cyclic peptides.[8] In contrast to the six- and seven-membered rings, the nine-membered ring is large enough to allow a linear N–H···O angle.

There may be an additional noncovalent attraction favoring the nine-membered-ring hydrogen-bonded triamide folding pattern. In the crystalline forms of **1**, **2**, and **4**, the C_{11}–N_{13} bond nearly eclipses the C_{10}–N_9 bond. This torsional arrangement places H_{13} very near N_9. The N_9···H_{13} distances of 2.36 (4) Å (**1**), 2.39 (4) Å (**2**), and 2.27 (4)/2.37 (4) Å (**4**) are at the edge of the range commonly used for crystallographic definition of hydrogen bonds.[14] The approach of H_{13} to N_9 corresponds to the direction in which the amide π electrons would be expected to occur, but the N_{13}–H_{13}···N_9 angles deviate substantially from linearity (107 (3)° (**1**), 110 (3)° (**2**), and 112 (3)°/111 (4)° (**4**)). Designation of the interaction between a hydrogen atom and an electronegative atom as a "hydrogen bond" implies the existence of an attraction between the two atoms; therefore, crystallographic data can never provide conclusive identification of hydrogen-bonding interactions.

However, even if the H_{13}···N_9 juxtapositions observed in **1**, **2**, and **4** do not correspond to interactions traditionally defined as hydrogen bonds, it seems likely that the antiparallel alignment of the N_{13}–H_{13} and C_{10}–N_9 bond dipoles is energetically favorable.

An interaction similar to those between H_{13} and N_9 in **1**, **2**, and **4** has been previously noted in the solid-state conformation of a 2-aminomalonic acid derivative.[19] In commenting on this structural feature, Gieren and Dederer suggested that such an interaction might play some role in determining protein folding patterns,[19,20] and Schäfer et al. have found support for this hypothesis in the results of ab initio calculations on *N*-acetylalanine *N'*-methylamide.[21] Lecomte et al. have remarked upon an analogous N—H···O(ester) interaction in the crystal structures of acetyl-L-prolyl-L-lactic acid methylamide and its D-lactyl diastereomer.[22] These depsipeptides adopt β-turn-like conformations containing a ten-membered-ring N—H···O=C interaction in the solid state. Alignment of the hydrogen-bond donor and acceptor for this primary interaction requires small lactate φ torsion angles (8° and 11°), which in each case places the C-terminal NH near the ester linkage's non-carbonyl oxygen. β-Turn conformations have been observed crystallographically in numerous small peptides, but the possible existence of a five-membered-ring N—H···N interaction across the residue in the $i + 2$ position does not appear to have been considered.[8] (In contrast, the five-membered-ring dipolar interaction that favors alignment of an amino acid residue's NH and the carbonyl of the same residue ("C_5 conformation") has been discussed at length.[23])

Comparison with Solution Data and Computational Predictions. The conformation observed for crystalline **1** corresponds to the intramolecular hydrogen-bonding pattern we have previously deduced, from spectroscopic data, to be most enthalpically stable for an isolated molecule in dilute methylene chloride solution. (The intermolecular hydrogen bonding detected in crystalline **1** does not occur under these solution conditions.) The conformations observed in the solid state for **2** and **4** match the folding pattern we have previously determined to be most favorable for the major rotamer of related triamide **9** in methylene chloride solution.[5]

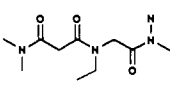

9

As previously reported for **9**,[5a] the NMR spectra of **2–4** in CD_2Cl_2 show evidence of slow rotation about the central tertiary amide C–N bond. NOE data indicate that the major solution rotamer of **9** has the *Z* configuration about this C–N bond,[5a] and we assign the major solution rotamers of **2–4** (≥85%) as *Z* by

(16) Peters, D.; Peters, J. *J. Mol. Struct.* **1980**, *68*, 255.
(17) Taylor, R.; Kennard, O. *J. Am. Chem. Soc.* **1982**, *104*, 5063.
(18) Milner-White, E. J.; Ross, B. M.; Ismail, R.; Belhadj-Mostefa, K.; Poet, R. *J. Mol. Biol.* **1988**, *204*, 777.
(19) Gieren, V. A.; Dederer, B. *Acta Crystallogr.* **1979**, *B34*, 533.
(20) Gieren, V. A.; Dederer, B.; Schanda, F. *Z. Naturforsch.* **1980**, *35c*, 741.
(21) Scarsdale, J. N.; Alsenoy, C. V.; Klimkowski, V. J.; Schäfer, L.; Momany, F. A. *J. Am. Chem. Soc.* **1983**, *105*, 3438.
(22) (a) Lecomte, C.; Aubry, A.; Protas, J.; Boussard, G.; Marraud, M. *Acta Crystallogr.* **1974**, *B30*, 1992. (b) Lecomte, C.; Aubry, A.; Protas, J.; Boussard, G.; Marraud, M. *Acta Crystallogr.* **1974**, *B30*, 2343.
(23) (a) Néel, J. *Pure Appl. Chem.* **1972**, *31*, 201. (b) Toniolo, C. *CRC Crit. Rev. Biochem.* **1980**, *9*, 1.

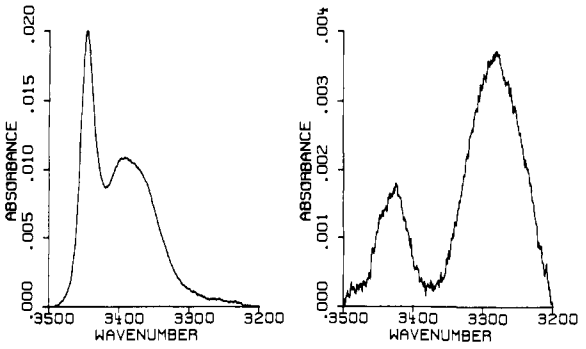

Figure 10. N–H stretch region of the FT-IR spectra for 1 mM diamide ester solutions in CH_2Cl_2 (room temperature), after subtraction of the spectrum of pure CH_2Cl_2. Data were obtained on a Nicolet 740 spectrometer: (a) diamide ester **5** (maxima at 3446 and 3394 cm^{-1}); (b) diamide ester **6** (maxima at 3431 and 3283 cm^{-1}). Note the difference in vertical scales.

analogy (only the *Z* configurations are observed crystallographically).

Figure 9 shows the N—H stretch regions of the IR spectra of **2–4** (1 mM each in CH_2Cl_2). There is only a small amount of non-hydrogen-bonded N—H stretch[24] in each case (maxima in the range 3430–3413 cm^{-1});[25] the major signals, 3298–3316 cm^{-1}, arise from amide NH groups engaged in intramolecular C=O···H—N hydrogen bonds. Previously reported experiments involving **9** have indicated that the intramolecular hydrogen bonds occurring in this family of molecules in solution involve the nine- rather than the seven-membered-ring C=O···H—N interaction.[5]

The unfolded conformation observed for **3** in the solid state is intriguing because the IR data indicate that this molecule adopts a nine-membered-ring hydrogen-bonded folding pattern almost exclusively in nonpolar solution.[26] IR data for diamide esters **5** and **6**, shown in Figure 10, also indicate that intramolecularly hydrogen-bonded conformations are highly populated in CH_2Cl_2, in contrast to the exclusively intermolecular hydrogen bonding observed in crystalline **5** and **6**. For **5**, the spectral data show substantial bands for both internally hydrogen-bonded and non-hydrogen-bonded N–H. The position of the hydrogen-bonded N–H maximum, 3394 cm^{-1}, suggests interaction with an ester acceptor;[4] conformations containing amide–amide hydrogen bonds, which generally give rise to bands ≤3360 cm^{-1}, do not appear to be highly populated in this case. (For example, the intramo-

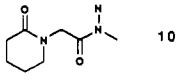
10

lecularly hydrogen-bonded N–H stretch band of diamide **10** in CH_2Cl_2 occurs at 3360 cm^{-1};[5a] the seven-membered-ring hydrogen bond available to **10** is similar to the seven-membered-ring amide–amide hydrogen bond available to **5**.) ^1H NMR data (not shown) suggest that intramolecular hydrogen bonding in **5** occurs largely in the six-membered ring rather than the nine-membered ring. For **6**, the major N–H stretch band occurs at 3283 cm^{-1}, implying extensive six-membered-ring hydrogen bonding under these conditions.

The most prominent intramolecular interaction among the crystal structures discussed here is the nine-membered-ring N—H···O=C interaction observed for **1**, **2**, and **4**. Molecular mechanics (AMBER/MacroModel)[27] and semiempirical (AM1)[28] calculations predict that the most stable conformations of an isolated molecule of **1** are those containing simultaneous six- and seven-membered-ring hydrogen bonds (**1a**) or simultaneous six- and nine-membered-ring hydrogen bonds (**1b**). Molecular mechanics calculations on triamide **9** predict that the global energy minimum for an isolated molecule contains only a seven-membered ring (**9a**).[27] Although these calculations are not designed to

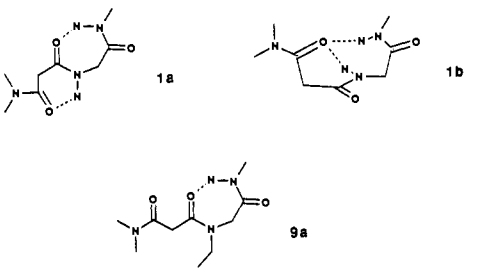
1a 1b

9a

reproduce the effects of the solid-state environment, it seems noteworthy that the folding patterns observed by diffraction for **1–4** are quite different from those predicted to be preferred computationally. (Since **2-4** differ from **9** only peripherally, we expect that calculations on **2–4** would give results similar to those reported for **9**.) In particular, no six- or seven-membered-ring hydrogen-bonding interactions were observed in any of the molecules we have examined crystallographically. As we have pointed out elsewhere,[29] careful comparison of reported computational results with experimental data for di- and triamides in methylene chloride solution indicates that the computational methods overemphasize the energetic benefit of hydrogen bonding in small rings.

Crystal Packing. The role played by intermolecular polar interactions, especially hydrogen bonds, in controlling crystal packing phenomena is a topic of continuing interest.[3,30] In a recent survey of small peptide crystal structures, Görbitz and Etter observed that the packing of such molecules tends to involve a segregation of polar and nonpolar moieties.[31] We undertook an examination of intermolecular organization in crystalline **2–4** in order to learn how these triamides' amphiphilicity affected their packing in the solid state.

Figure 11 shows the arrangement of triamide **2** in the solid state, as viewed down the *y* axis. The crystal is composed of alternating polar and nonpolar sheets that lie approximately in the *xy* plane. Each polar sheet has a thickness of two *N*-malonylglycine moieties, and each nonpolar sheet has a thickness of two phenyl rings. The juxtaposition of the phenyl rings in each nonpolar sheet corresponds to the "herringbone" pattern that is observed in the crystal lattices of many aromatic hydrocarbons.[32] Figure 12 presents this phenyl ring packing pattern from a different perspective and in more detail.

The association of the triamide portions of **2** occurring in the solid state presumably results at least in part from favorable interactions among the amide dipoles.[33] Such dipolar interactions can be energetically substantial, but this type of dipole–dipole attraction is not as readily identified by visual inspection as are hydrogen bonds because the connection between the spatial re-

(24) We use the term "non-hydrogen-bonded" to signify the absence of an N—H···O=C interaction. Such protons in methylene chloride are presumably engaged in weak interactions with the solvent.

(25) Experiments with **9** have suggested that the small band in the non-hydrogen-bonded N–H stretch region of the IR spectrum arises largely from the minor rotamer about the central C–N bond; see ref 4, note 22.

(26) Other examples are known in which a molecule displays different conformations in the crystalline and solution states. See, for example: Kessler, H.; Zimmermann, G.; Fôrster, H.; Engel, J.; Oepen, G.; Sheldrick, W. S. *Angew. Chem., Int. Ed. Engl.* **1981**, *20*, 1053.

(27) (a) Smith, D. A.; Vijayakmuar, S. *Tetrahedron Lett.* **1991**, *32*, 3613. (b) Smith, D. A.; Vijayakmuar, S. *Tetrahedron Lett.* **1991**, *32*, 3617.

(28) Novoa, J. J.; Whangbo, M.-H. *J. Am. Chem. Soc.* **1991**, *113*, 9017.

(29) (a) Gellman, S. H.; Dado, G. P. *Tetrahedron Lett.* **1991**, *32*, 7377. (b) Dado, G. P.; Gellman, S. H. *J. Am. Chem. Soc.* **1992**, *114*, 3138.

(30) For leading references, see: (a) Simard, M.; Su, D.; Wuest, J. D. *J. Am. Chem. Soc.* **1991**, *113*, 4696. (b) Xhao, X.; Chang, Y.-L.; Fowler, F. W.; Lauher, J. W. *J. Am. Chem. Soc.* **1990**, *112*, 6627. (c) Zerkowski, J. A.; Seto, C. T.; Wierda, D. A.; Whitesides, G. M. *J. Am. Chem. Soc.* **1990**, *112*, 9025. (d) Lehn, J.-M.; Mascal, M.; DeCian, A.; Fischer, J. *J. Chem. Soc., Chem. Commun.* **1990**, 479.

(31) Görbitz, C. H.; Etter, M. C. *Int. J. Peptide Protein Res.*, in press.

(32) Desiraju, G. R.; Gavezzotti, A. *Acta Crystallogr.* **1989**, *B45*, 473 and references therein.

(33) (a) Leiserowitz, L.; Hagler, A. T. *Proc. R. Soc. London A* **1983**, *388*, 133. (b) Dauber, P.; Hagler, A. T. *Acc. Chem. Res.* **1980**, *13*, 105.

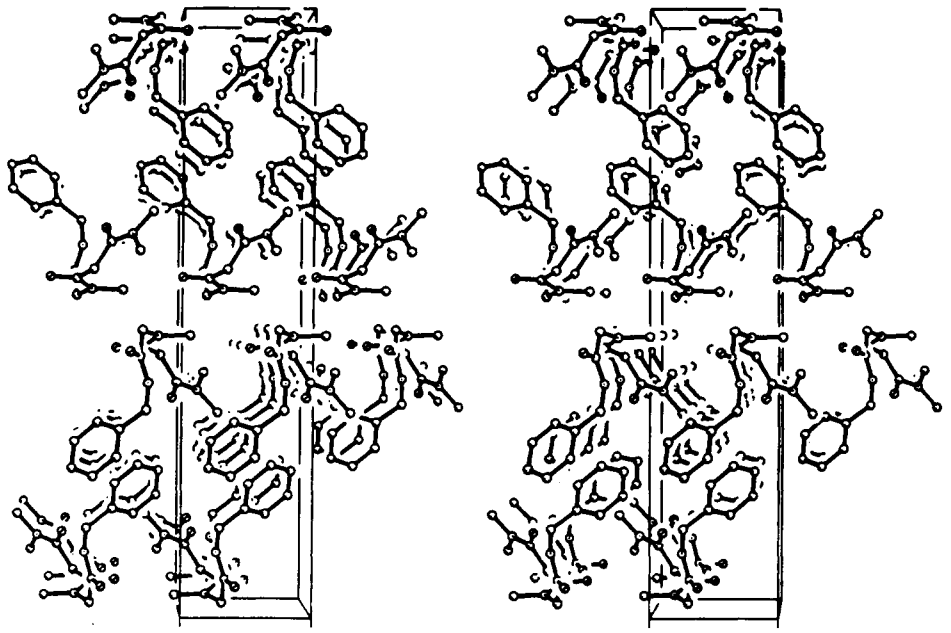

Figure 11. Crystal packing of triamide 2 (stereoview) viewed down the y axis.

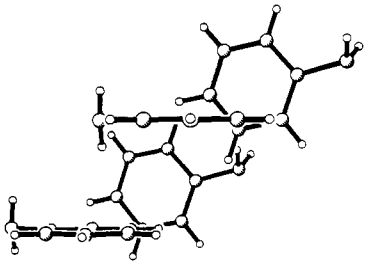

Figure 12. Detail of the crystal packing of triamide 2, showing the "herringbone" arrangement of neighboring phenyl rings.

lationship of any pair of amide groups and their energy of interaction is not as simple as for hydrogen bonding.[34] Intermolecular juxtapositions involving the tertiary amide group containing N_9—C_7=O_8 seem especially likely to be attractive in this packing arrangement. Linear head-to-tail arrays of these tertiary amide groups occur within the polar sheets, running approximately along the x axis (left to right in Figure 11); this orientation may provide an attraction between neighbors in the x direction. The two halves of each polar sheet come together in an offset parallel stacking of these head-to-tail arrays against one another. The offset arrangement may lead to a net dipolar attraction between the two halves of the polar sheets.

Figure 13 shows the crystal packing of 3, viewed along the y axis. Although the conformation of the triamide fragment of 3 is different from the conformation of the analogous subunit of 2, the crystal of 3, like the crystal of 2, is composed of alternating polar and nonpolar sheets, lying approximately in the xy plane. The polar sheets of 3 have a thickness of only one N-malonylglycine moiety, in contrast to the pattern occurring in 2. The nonpolar sheets of 3 have a thickness of two naphthyl groups, which congregate in a herringbone pattern; the naphthyl–naphthyl arrangment is presented from a different perspective and in more detail in Figure 14.

In addition to the C_{10}—H_{10}···O_8=C_7 interaction discussed above, crystalline 3 appears to contain a second intermolecular C—H···O hydrogen bond,[17] involving O_5 and H_{16} (H···O = 2.36 (5) Å; H_{16} was independently refined). Both of the C_{16}–H_{16}···O_5=C_4 interactions experienced by a given molecule occur with a single partner (i.e., each molecule interacts with H_{16} and O_5 of the same neighbor), and these interactions occur approximately along the z axis. For a given molecule of 3, the C_{16}—H_{16}···O_5 partner occurs in the same "translational stack" (along the y axis) as the N—H···O partner, and these C—H···O and N—H···O partners of a given triamide molecule are themselves nearest neighbors within their translational stack.

Figure 15 shows the crystal packing of triamide 4, viewed along the y axis. The arrangement of molecules in this lattice is quite different from the arrangement observed for 2 or 3, but a pattern of alternating polar and nonpolar sheets is achieved by 4 nevertheless. The plane containing these sheets is defined by the y axis and an axis lying approximately on the diagonal between the x and z axes. The nonpolar sheet has a thickness of one adamantyl moiety, and the polar sheet has a thickness of one N-malonylglycine moiety.

Several short intermolecular C–H···O contacts in crystalline 4 are identified as hydrogen bonds by the criterion of O···H < 2.4 Å.[17] For each of the two crystallographically independent molecules, O_8 makes a close approach to one of the hydrogens on C_{10} of an adjacent molecule, with O···H distances of 2.243 (5) and 2.307 (5) Å. These hydrogen bonds are roughly parallel to the y axis. For one of the crystallographically independent molecules, O_{12} is quite close to one of the hydrogens on C_6 of a neighbor (2.199 (5) Å). (None of the hydrogen atoms involved in these intermolecular interactions was refined independently.)

Crystal structures of soluble proteins commonly reveal a segregation of polar and nonpolar amino acid side chains between exterior and interior regions, respectively.[1] The interior location of nonpolar side chains is often attributed to the operation of the hydrophobic effect.[1] Since 2–4 were crystallized by vapor diffusion of hexane into 1,2-dichloroethane solutions of the triamides, the segregation of polar and nonpolar fragments in their crystals cannot be a manifestation of the hydrophobic effect, but must instead reflect the intrinsic organizational preferences of the fragments themselves.

Conclusion. The data presented here provide insight on the forces that control the folding of molecules containing the N-malonylglycine unit and on the forces that control the packing of such molecules into the crystalline state. Three of the six molecules examined crystallographically display a folded conformation that contains a nine-membered-ring N—H···O=C hydrogen bond. These observations suggest that the nine-membered-ring conformation is intrinsically favorable to the N-malonylglycine unit, a conclusion that is consistent with our interpretation of spectroscopic data for 1–4 and the related molecule 9 in nonpolar solution.[5] The data also suggest that there may be

(34) For recent discussions of the geometrical aspects of dipole–dipole interactions in crystal packing, see: (a) Gavezzotti, A. *J. Phys. Chem.* **1990**, *94*, 4319. (b) Whitesell, J. K.; Davis, R. E.; Saunders, L. L.; Wilson, R. J.; Feagins, J. P. *J. Am. Chem. Soc.* **1991**, *113*, 3267.

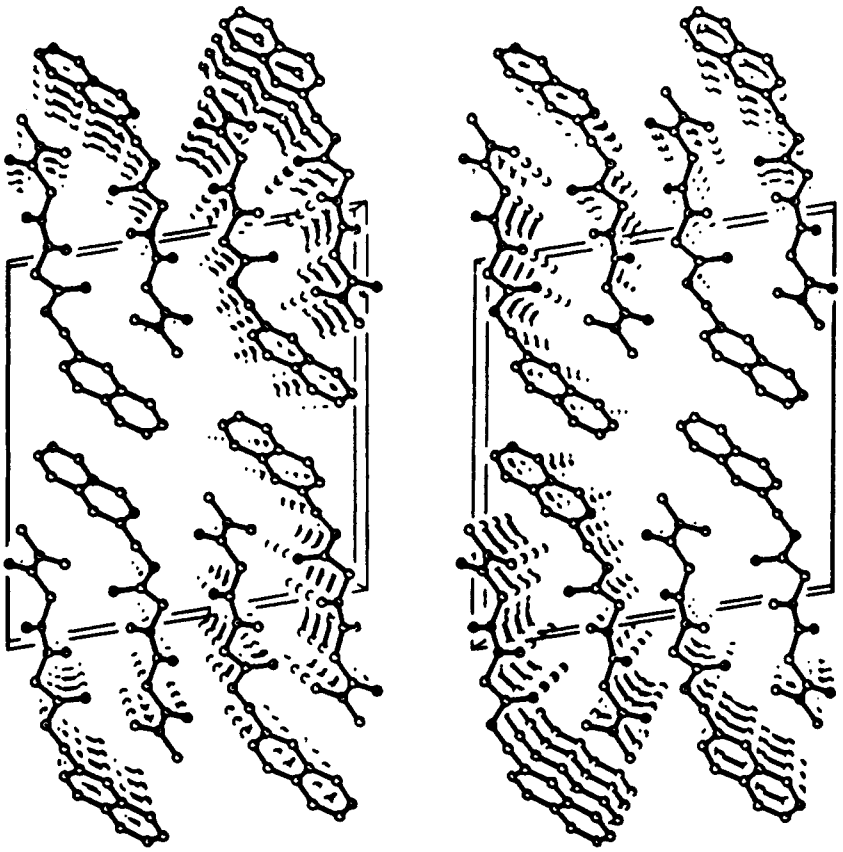

Figure 13. Crystal packing of triamide **3** (stereoview) viewed down the *y* axis.

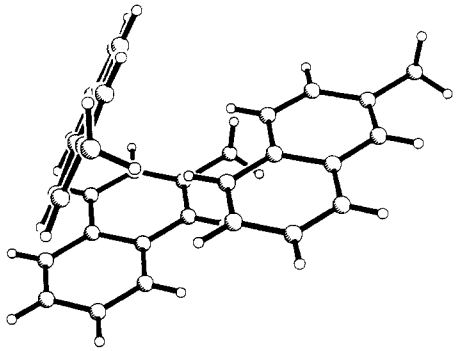

Figure 14. Detail of the crystal packing of triamide **3**, showing the "herringbone" arrangement of the neighboring naphthyl groups.

a second weak dipolar attraction at work within the folded conformations observed for **1**, **2**, and **4**. In each case, the amide proton involved in the nine-membered-ring C=O···H—N interaction also approaches the glycine nitrogen atom. Because the N—H···N geometry is poor, it may be inappropriate to designate this five-membered-ring interaction as a "hydrogen bond," but this arrangement does appear to provide a favorable alignment of N—H and C—N bond dipoles. It should be stressed that the crystallographic detection of one and possibly two attractive dipolar interactions within the folded conformations of these triamides does not necessarily imply that these dipolar interactions are the principal conformation-determining forces at work within these molecules. We have previously shown that the combination of torsional potentials along the backbone of the *N*-malonylsarcosine unit predisposes molecules **2–4** to adopt folded conformations in solution, relative to analogous but more flexible backbones.[5c]

Comparison of the crystal packing patterns of analogous triamides **2–4** reveals an intriguing consistency. All three arrange themselves to produce alternating sheets of polar and nonpolar moieties, despite the different molecular conformation of **3** relative to **2** and **4** and despite the variations in the juxtaposition of neighbors. Further study of this segregration in crystals of amphiphilic molecules should provide insight on the forces that control the interior packing of folded proteins and long-range order in the solid state.

Experimental Section

All melting points are uncorrected. THF was freshly distilled from sodium benzophenone ketyl under N_2. Triethylamine and DMF were distilled before use. ^1H NMR spectra were obtained on a Bruker WP-200 spectrometer. Dicyclohexylcarbodiimide (DCC) and *N*-hydroxysuccinimide were used as obtained from Aldrich Chemical Co. For Boc removal, 4N HCl in dioxane from Pierce Chemical Co. was used. FT-IR spectra were obtained on a Nicolet 740 instrument. IR solution samples were prepared under N_2 (glove bag) in freshly distilled CH_2Cl_2; the compounds used to prepared IR samples were judged to be >90% pure by high-resolution ^1H NMR spectroscopy. High-resolution electron impact ionization mass spectroscopy was performed on a Kratos MS-80. Column chromatography was carried out using low N_2 pressure with 230–400 mesh silica gel 60 from EM Science. Columns eluted with low percentages of MeOH in $CHCl_3$ were slurry-packed after the slurry had been stirred with the eluant for at least 1 h. Fresh solvent was then passed through the column continuously until subtle changes in the gray hue of the silica had moved completely through the column bed (for 2% MeOH or less, this preequilibration of the column could be quite time-consuming). Preequilibration was essential for optimal resolution.

Triamide 1. To a solution of 1.5 g (11.5 mmol) of the mono-*N*,*N*-dimethylamide of malonic acid[4] in 60 mL of THF were added 1.98 g (17.3 mmol) of *N*-hydroxysuccinimide and 2.97 g (14.4 mmol) of DCC; a white precipitate quickly formed. After this mixture had been stirred under N_2 for 2 h, a mixture of 4 mL of triethylamine and solid glycine methylamide hydrochloride (obtained from reaction of 2.16 g (11.5 mmol) of *N*-(*tert*-butyloxycarbonyl)glycine *N'*-methylamide with 10 mL of 4 N HCl in dioxane; the dioxane was removed before subsequent reaction) in 90 mL of DMF was added. The resulting slurry was stirred under N_2 for 22 h. The precipitate was then removed by gravity filtration. After concentration of the filtrate, the crude product was purified by SiO_2 column chromatography eluting with 5–7% MeOH in $CHCl_3$ to afford slightly impure material in 63% yield. Recrystallization from hexane/CH_2Cl_2 afforded 0.86 g (37% yield) of triamide **1** as a white crystalline solid: mp 123–126 °C; ^1H NMR ($CDCl_3$) δ 7.81 (broad triplet, 1 H, NH), 7.07 (broad, 1 H, NH), 3.94 (d, J = 6.1 Hz, 2 H, $NHCH_2$), 3.37 (s, 2 H, $(C{=}O)_2CH_2$), 3.05 (s, 3 H, NCH_3), 2.98 (s, 3 H, NCH_3), 2.79 (d, J = 4.8 Hz, 3 H, $NHCH_3$); ^{13}C NMR ($CDCl_3$) δ

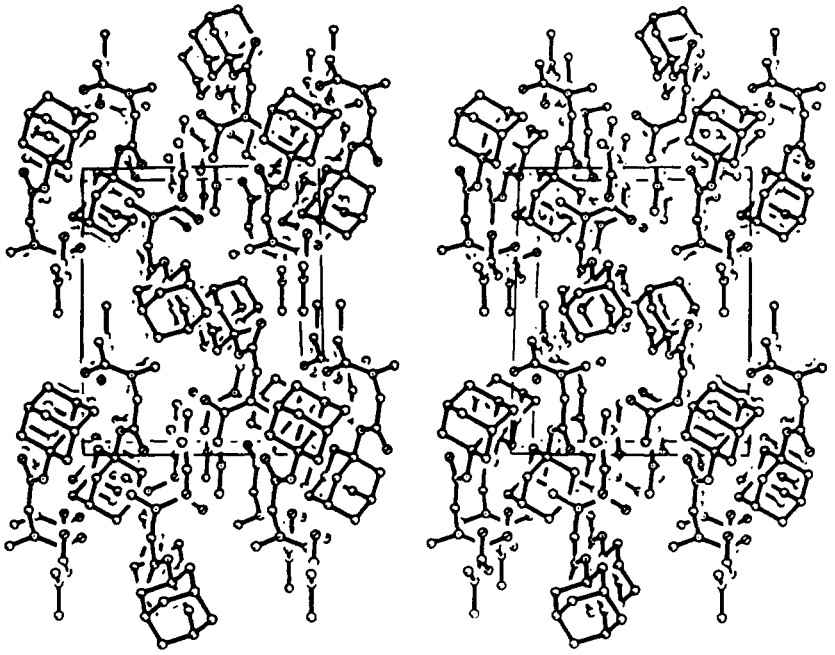

Figure 15. Crystal packing of triamide **4** (stereoview) viewed down the *y* axis.

169.5, 168.1, 167.3, 43.4, 40.3, 37.6, 35.7, 26.2; IR (0.001 M in CH_2Cl_2) 3444 (NH), 3316 (NH), 1675 (amide I), 1638 (amide I), 1558 (amide II), 1522 (amide II) cm^{-1}; EI MS *m/e* obsd 201.1111, calcd for $C_8H_{15}N_3O_3$ 201.1113.

***N*-(*tert*-Butyloxycarbonyl)sarcosine *N'*-Benzylamide.** To a solution of 0.54 g (2.86 mmol) of *N*-(*tert*-butyloxycarbonyl)sarcosine in 19 mL of THF were added 0.46 g (4 mmol) of *N*-hydroxysuccinimide and 0.64 g (3.11 mmol) of DCC; a precipitate quickly formed. After this mixture had been stirred for 1.5 h under N_2, 0.31 mL (2.9 mmol) of benzylamine was added and the mixture was stirred under N_2 for 21 h. Solids were then removed by gravity filtration. After concentration of the filtrate, the crude product was purified by SiO_2 chromatography with 2–5% MeOH in $CHCl_3$ to afford 0.63 g (80% yield) of the desired benzylamide as a white solid: mp 76–79 °C; ^1H NMR ($CDCl_3$) δ 7.29 (m, 5 H, aromatic CH), 6.35 (broad, 1 H, NH), 4.47 (d, J = 5.9 Hz, 2 H, $ArCH_2$), 3.91 (s, 2 H, CH_2), 2.94 (s, 3 H, NCH_3), 1.41 (s, 9 H, $C(CH_3)_3$); IR (CH_2Cl_2) 3431 (NH), 2933 (CH), 1683 (amide I), 1522 (amide II) cm^{-1}; EI MS *m/e* obsd 222.1012, calcd for $C_{11}H_{14}N_2O_3$ ($M^+ - C_4H_8$) 222.1004.

***N*-(*tert*-Butyloxycarbonyl)sarcosine *N'*-(2-naphthylmethyl)amide** was prepared from *N*-(*tert*-butyloxycarbonyl)sarcosine and (2-naphthylmethyl)amine by an analogous procedure. The desired amide was isolated by SiO_2 chromatography with 2% MeOH in $CHCl_3$ as a pale yellow solid in 95% yield: mp 74–76 °C; ^1H NMR ($CDCl_3$) δ 7.9–7.4 (m, 7 H, aromatic CH), 6.6 (broad, 1 H, NH), 4.70 (d, J = 7.0 Hz, 2 H, $ArCH_2$), 3.95 (s, 2 H, CH_2), 2.94 (s, 3 H, CH_3), 1.40 (s, 9 H, $C(CH_3)_3$); IR (CH_2Cl_2) 3431 (NH), 2936 (CH), 1685 (amide I), 1522 (amide II); EI MS *m/e* obsd 272.1146, calcd for $C_{15}H_{16}N_2O_3$ ($M^+ - C_4H_8$) 272.1161.

***N*-(*tert*-Butyloxycarbonyl)sarcosine *N'*-1-adamantylamide** was prepared in an analogous manner from *N*-(*tert*-butyloxycarbonyl)sarcosine and 1-adamantylamine. Purification by SiO_2 chromatography afforded the desired amide as a white solid in 67% yield: mp 114.5–115.5 °C; ^1H NMR ($CDCl_3$) δ 5.6 (broad, 1 H, NH), 3.72 (s, 2 H, NCH_2CO), 2.92 (s, 3 H, NCH_3), 2.08 (s, 3 H, CH_2CH), 1.99 (s, 6 H, $NHCCH_2$), 1.68 (s, 6 H, $CHCH_2$), 1.48 (s, 9 H, $C(CH_3)_3$); IR (CH_2Cl_2) 3413 (NH), 2913 (CH), 1694 (amide I), 1683 (amide I), 1520 (amide II) cm^{-1}; EI MS *m/e* obsd 322.2262, calcd for $C_{18}H_{30}N_2O_3$ 322.2256.

Triamide 2 was prepared from *N*-(*tert*-butyloxycarbonyl)sarcosine *N'*-benzylamide in a procedure analogous to the preparation of triamide **1**. The desired amide was isolated by SiO_2 chromatography with 2% MeOH in $CHCl_3$ as a white solid in 93% yield: mp 101–102 °C; ^1H NMR ($CDCl_3$) major rotamer (>85%) δ 8.45 (broad, 1 H, NH), 7.32–7.26 (m, 5 H, aromatic CH), 4.47 (d, J = 5.8 Hz, 2 H, $ArCH_2$), 4.15 (s, 2 H, NCH_2CO), 3.54 (s, 2 H, CH_2), 3.02 (s, 3 H, NCH_3), 2.99 (s, 3 H, NCH_3), 2.90 (s, 3 H, NCH_3), minor rotamer (<15%) δ 4.05 (s, 2 H, NCH_2CO), 2.85 (s, 3 H, NCH_3); IR (0.001 M in CH_2Cl_2) 3430 (NH), 3299 (NH), 1663 (amide I), 1639 (amide I), 1545 (amide II) cm^{-1}; EI MS *m/e* obsd 291.1589, calcd for $C_{15}H_{21}N_3O_3$ 291.1583.

Triamide 3 was prepared in an analogous manner from *N*-(*tert*-butyloxycarbonyl)sarcosine *N'*-(2-naphthylmethyl)amide. Purification by SiO_2 chromatography with 2% MeOH in $CHCl_3$ afforded the desired triamide as a white solid in 72% yield: mp 134–135 °C; ^1H NMR ($CDCl_3$) major rotamer (>85%) δ 8.52 (broad t, J = 6 Hz, 1 H, NH), 7.8–7.4 (m, 7 H, aromatic CH), 4.63 (d, J = 5.9 Hz, 2 H, $ArCH_2$), 4.16 (s, 2 H, NCH_2CO), 3.50 (s, 2 H, CH_2), 2.98 (s, 3 H, NCH_3), 2.93 (s, 3 H, NCH_3), 2.79 (s, 3 H, NCH_3), minor rotamer (<15%) δ 4.1 (s, 2 H, NCH_2CO), 2.96 (s, 3 H, NCH_3), 2.81 (s, 3 H, NCH_3); IR (0.001 M in CH_2Cl_2) 3430 (NH), 3298 (NH), 1663 (amide I), 1639 (amide I), 1545 (amide II) cm^{-1}; EI MS *m/e* obsd 341.1734, calcd for $C_{19}H_{23}N_3O_3$ 341.1739.

Triamide 4 was prepared in an analogous manner from *N*-(*tert*-butyloxycarbonyl)sarcosine *N'*-1-adamantylamide. The triamide was isolated as a white solid in 88% yield after purification by SiO_2 chromatography with 4% MeOH in $CHCl_3$: mp 126–128 °C; ^1H NMR ($CDCl_3$) major rotamer (~85%) δ 6.94 (broad, 1 H, NH), 4.00 (s, 2 H, NCH_2CO), 3.54 (s, 2 H, CH_2), 3.03 (s, 6 H, $N(CH_3)_2$), 2.99 (s, 3 H, NCH_3), 2.06 (s, 6 H, $NHCCH_2$), 2.02 (s, 3 H, CH_2CH), 1.67 (s, 6 H, $CHCH_2$), minor rotamer (~15%) δ 6.75 (broad, 1 H, NH), 3.92 (s, 2 H, NCH_2CO), 3.10 (s, 3 H, NCH_3); IR (0.001 M in CH_2Cl_2) 3413 (NH), 3316 (NH), 1661 (amide I), 1642 (amide I), 1538 (amide II) cm^{-1}; EI MS *m/e* obsd 335.2219, calcd for $C_{18}H_{29}N_3O_3$ 335.2209.

Ester Diamide 5. To 0.38 g (2 mmol) of *N*-(*tert*-butyloxycarbonyl)-glycine *N'*-methylamide was added 5 mL of 4 N HCl in dioxane. The mixture was stirred under N_2 for 1 h, and then excess HCl was removed by bubbling a stream of N_2 through the mixture for 20 min. Dioxane was removed by rotary evaporation to afford glycine methylamide hydrochloride as a white solid. This material was dissolved in 10 mL of DMF, and 0.7 mL of triethylamine was added, followed by a solution of 0.27 g (2 mmol) of methylmalonyl chloride in 10 mL of DMF. After this mixture was stirred under N_2 for 7 h, the suspended solids were removed by gravity filtration, and the filtrate was concentrated. The crude product was purified by SiO_2 chromatography with 5% MeOH in $CHCl_3$ followed by recrystallization from chloroform and hexane to afford 0.074 g (27% yield) of the desired ester diamide as a white crystalline solid: mp 142.5–143.5 °C; ^1H NMR ($CDCl_3$) δ 7.57 (broad, 1 H, $NHCH_2$), 6.42 (broad, 1 H, $NHCH_3$), 3.95 (d, J = 5.5 Hz, 2 H, $NHCH_2CO$), 3.76 (s, 3 H, OCH_3), 3.38 (s, 2 H, CH_2), 2.82 (d, J = 4.8 Hz, 3 H, $NHCH_3$); ^{13}C NMR ($CDCl_3$) δ 169.4, 169.0, 165.6, 52.8, 52.5, 42.4, 41.2; IR (0.001 M in CH_2Cl_2) 3446 (NH), 3395 (NH), 1727 (ester C=O), 1678 (amide I), 1523 (amide II) cm^{-1}; EI MS *m/e* obsd 189.0864, calcd for $C_7H_{12}N_2O_4$ (M^+ + H) 189.0875.

Ester diamide 6 was prepared from *N*-(*tert*-butyloxycarbonyl)glycine methyl ester in a procedure analogous to the preparation of triamide **1**. The desired product was purified by SiO_2 chromatography with 2% MeOH in $CHCl_3$; recrystallization from dichloroethane/hexane gave **6** as a white crystalline solid in 47% yield: mp 144.5–145.5 °C; ^1H NMR ($CDCl_3$) δ 8.43 (broad, 1 H, NH), 4.06 (d, J = 5.5 Hz, 2 H, $NHCH_2CO$), 3.75 (s, 3 H, OCH_3), 3.37 (s, 2 H, CH_2), 3.07 (s, 3 H, NCH_3), 2.99 (s, 3 H, NCH_3); ^{13}C NMR ($CDCl_3$) δ 169.9, 168.1, 166.6, 52.2, 41.1, 39.3, 37.7, 35.7; IR (0.001 M in CH_2Cl_2) 3423 (NH), 3279

(NH), 1751 (ester C=O), 1675 (amide I), 1633 (amide I), 1536 (amide II), 1500 (amide II) cm^{-1}; EI MS m/e obsd 202.0954, calcd for $C_8H_{14}N_2O_4$ 202.0954.

Growth of Crystals for Diffraction Studies. Prisms of triamide **1** were obtained by dissolving the material in hot CH_2Cl_2, adding hexane to saturation, and allowing the solution to cool to room temperature. Thin plates of **2** and **5** were grown by vapor diffusion of hexane into 1,2-dichloroethane solutions of the compounds at room temperature; the same procedure afforded prisms of **3**. Plates of **4** were obtained by vapor diffusion of hexane into a 1,2-dichloroethane of the triamide at -20 °C. Thin plates of **6** were grown by slow evaporation of a hexane/1,2-dichloroethane solution at room temperature.

Acknowledgment. We thank Professors M. C. Etter and M.-H. Whangbo for sharing results with us prior to publication. This research was supported, in part, by the donors of the Petroleum Research Fund, administered by the American Chemical Society, and by the National Science Foundation (CHE-9014488). The FT-IR spectrometer was purchased with funds provided by the Office of Naval Research (N00014-90-J-1902). G.P.D. is the recipient of a National Research Service Award (T32 GM08923) from the National Institute of General Medical Sciences, and C.J.R. is the recipient of a fellowship from the Graduate School of the University of Wisconsin—Madison. S.H.G. thanks the Searle Scholars Program, the American Cancer Society (Junior Faculty Research Award), the National Science Foundation Presidential Young Investigator Program (CHE-9157510), the Eastman Kodak Company, and the Upjohn Company for support.

Note Added in Proof. Collins et al. (*Inorg. Chem.* **1991**, *30*, 4204) have very recently reported the crystal structure of a macrocyclic tetraamide that contains multiple *N*-malonylglycine skeletal units. In the solid state, this macrocycle displays two interwoven nine-membered-ring C=O···H—N hydrogen bonds.

Supplementary Material Available: Listings of literature references for crystal structures of malonamide derivatives and crystallographic details for **1-6**, including tables of atomic coordinates and bond lengths and angles (44 pages); listing of observed and calculated structure factors (45 pages). Ordering information is given on any current masthead page.

Size and Location of Cobalt Clusters in Zeolite NaY: A Nuclear Magnetic Resonance Study§

Z. Zhang,† Y. D. Zhang,‡ W. A. Hines,*,‡ J. I. Budnick,‡ and W. M. H. Sachtler†

Contribution from Ipatieff Laboratory, Department of Chemistry, Northwestern University, Evanston, Illinois, 60208, and Department of Physics and Institute of Materials Science, University of Connecticut, Storrs, Connecticut 06269. *Received November 27, 1991*

Abstract: In this work, it is demonstrated how information concerning the size and location of Co clusters in the zeolite NaY can be obtained by measurements of the ^{59}Co spin-echo NMR spectrum. The critical temperature for the superparamagnetic/ferromagnetic transition was used to obtain an estimate for the average cluster size in Co/NaY samples which were prepared using different thermal treatments. In addition, a selective chemical treatment with triphenylphosphine was used to determine the location of the clusters. It was found that preparation of Co/NaY under "mild" conditions (decomposition and annealing carried out at 200 °C) resulted in the production of Co clusters with an average diameter of 6-10 Å inside the NaY cages, while preparation of Co/NaY under "extreme" conditions (decomposition and annealing carried out at 500 °C) resulted in larger clusters outside the NaY cages.

I. Introduction

Volatile transition metal complexes have been widely used for the production of zeolite-encaged metal catalysts.[1,2] For the first-row transition metals that are difficult to reduce from ionic precursors, severe reduction conditions can be avoided by using appropriate volatile precursors. Most carbonyl complexes can be introduced into zeolite cages via the vapor phase. They remain intact at low temperature and under CO pressure.[3,4] However, at elevated temperature or in vacuo, they decompose by releasing CO ligands. In the preparation of zeolite-supported Co catalysts, Co carbonyl [$Co_2(CO)_8$] is frequently used.[5,6] Since Co^{2+} ions in zeolite Y cannot be reduced below 750 °C,[7,8] the use of the volatile $Co_2(CO)_8$ precursor is advantageous because it decomposes at low temperature, leading to highly dispersed Co particles. In situ far-IR spectroscopy has shown that adsorbed $Co_2(CO)_8$ interacts with the accessible supercage cations in the NaY and CoY zeolites.[9] In the zeolite HY, Co atoms are oxidized to Co^{2+} ions by the zeolite protons. Therefore, the acidic form of zeolite is to be avoided. The final dispersion of Co in the zeolite cages is determined not only by the decomposition technique[10-12] but also by the properties of the zeolite supports and by the method with which the Co carbonyl complex is introduced into the zeolites. In this study, ^{59}Co nuclear magnetic resonance (NMR) spectroscopy has been utilized to determine the size and location of

§ We thank the National Science Foundation (Grant No. CTS11184) and the University of Connecticut Research Foundation for supporting this work.

† Northwestern University.

‡ University of Connecticut.

(1) Yermakov, Y. I.; Kuznetsov, B. N.; Zakharov, V. A. *Catalysis by Supported Complexes*; Elsevier: Amsterdam, 1981.
(2) Gates, B. C.; Guczi, L.; Knözinger, H. *Metal Clusters in Catalysis*; Elsevier: Amsterdam, 1986.
(3) Okamoto, Y.; Inui, Y.; Onimatsu, H.; Imanaka, T. *J. Phys. Chem.* **1991**, *95*, 4596.
(4) Maloney, S. D.; Zhou, P. L.; Kelly, M. J.; Gates, B. C. *J. Phys. Chem.* **1991**, *95*, 5409.
(5) Schneider, R. L.; Howe, R. F.; Watters, K. L. *Inorg. Chem.* **1984**, *23*, 4600.
(6) Connaway, M. C.; Hanson, B. E. *Inorg. Chem.* **1986**, *25*, 1445.
(7) Zhang, Z.; Sachtler, W. M. H. *J. Chem. Soc., Faraday Trans.* **1990**, *86*, 2313.
(8) Zhang, Z.; Sachtler, W. M. H.; Suib, S. L. *Catal. Lett.* **1989**, *2*, 395.
(9) Ozin, G. A.; Godber, J. P. Intrazeolite Organometallics: Spectroscopic Probes of Internal versus External Confinement of Metal Clusters. In *Excited States and Reactive Intermediates: Photochemistry, Photophysics and Electrochemistry*; Lever, A. B. P., Ed.; ACS Symposium Series 307; American Chemical Society: Washington, DC, 1986.
(10) Lewis, K. E.; Golden, D. M.; Smith, G. P. *J. Am. Chem. Soc.* **1984**, *106*, 3905.
(11) Zerger, R. P.; McMahon, K. C.; Michel, R. G.; Seltzer, M. D.; Suib, S. L. *J. Catal.* **1986**, *99*, 498.
(12) Zhang, Z.; Suib, S. L.; Zhang, Y. D.; Hines, W. A.; Budnick, J. I. *J. Am. Chem. Soc.* **1988**, *110*, 5569.

0002-7863/92/1514-4843$03.00/0